Inhibition of the glucocorticoid-activating enzyme 11β-hydroxysteroid dehydrogenase type 1 drives concurrent 11-oxygenated androgen excess

Lina Schiffer[1,#], Imken Oestlund[2,#], Jacky Snoep[2,3], Lorna C. Gilligan[1], Angela E. Taylor[1], Alexandra J. Sinclair[1], Rishi Singhal[4], Adrian Freeman[5], Ramzi Ajjan[6,7], Ana Tiganescu[6,7], Wiebke Arlt[1,8,9] and Karl-Heinz Storbeck[1,2]

[1] Institute of Metabolism and Systems Research, University of Birmingham, Birmingham, UK

[2] Department of Biochemistry, Stellenbosch University, Stellenbosch, South Africa

[3] Molecular Cell Physiology, Vrije Universiteit Amsterdam, Amsterdam, The Netherlands

[4] Upper GI Unit and Minimally Invasive Unit, Heartlands Hospital, University Hospitals Birmingham NHS Foundation Trust, Birmingham, UK

[5]Emerging Innovations Unit, Discovery Sciences, BioPharmaceuticals R&D, AstraZeneca, Cambridge, UK

[6] Leeds Institute of Cardiovascular and Metabolic Medicine, University of Leeds, Leeds, UK

[7] NIHR Leeds Biomedical Research Center, Leeds Teaching Hospitals, NHS Trust, Leeds, UK

[8] Institute of Clinical Sciences, Faculty of Medicine, Imperial College, London, UK

[9] Medical Research Council London Institute of Medical Sciences, London, UK

[#]Shared first authors.

Conflict-of-interest: The authors have declared that no conflict of interest exists.

Abstract

Aldo-keto reductase 1C3 (AKR1C3) is a key enzyme in the activation of both classic and 11-oxygenated androgens. In adipose tissue, AKR1C3 is co-expressed with 11β-hydroxysteroid dehydrogenase type 1 (HSD11B1), which catalyses the local activation of glucocorticoids but also the inactivation of 11-oxygenated androgens, and thus has the potential to counteract AKR1C3. Using a combination of *in vitro* assays and *in silico* modelling we show that HSD11B1 attenuates the biosynthesis of the potent 11-oxygenated androgen, 11-ketotestosterone, by AKR1C3. Employing *ex vivo* incubations of human female adipose tissue samples we show that inhibition of HSD11B1 results in the increased peripheral biosynthesis of 11-ketotestosterone. Moreover, circulating 11KT increased 2-3 fold in individuals with type 2 diabetes after receiving the selective oral HSD11B1 inhibitor AZD4017 for 35 days, thus confirming that HSD11B1 inhibition results in systemic increases in 11KT concentrations. Our findings show that HSD11B1 protects against excess 11KT production by adipose tissue, a finding of particular significance when considering the evidence for adverse metabolic effects of androgens in women. Therefore, when targeting glucocorticoid activation by HSD11B1 inhibitor treatment in women, the consequently increased generation of 11-ketotestosterone may offset beneficial effects of decreased glucocorticoid activation.

39 **Graphical Abstract**

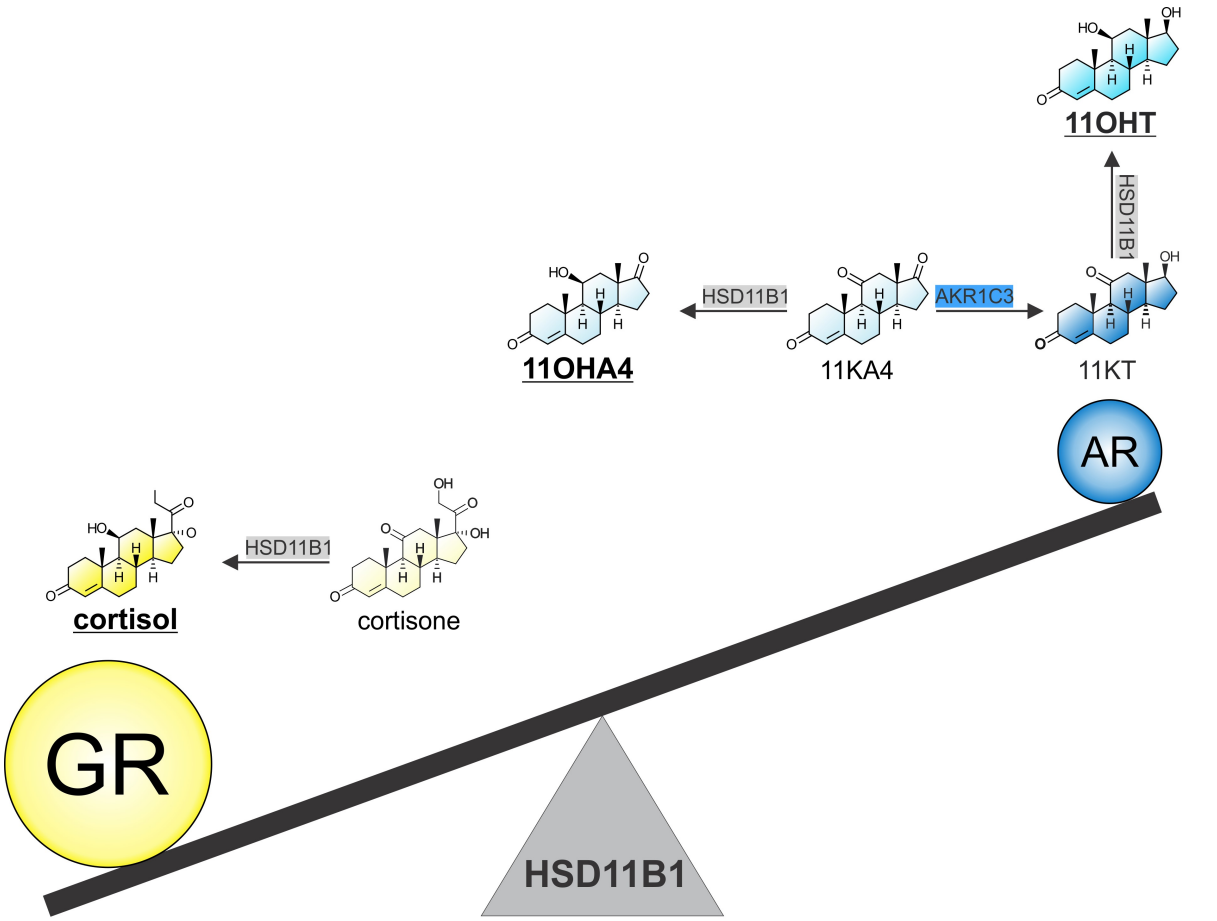

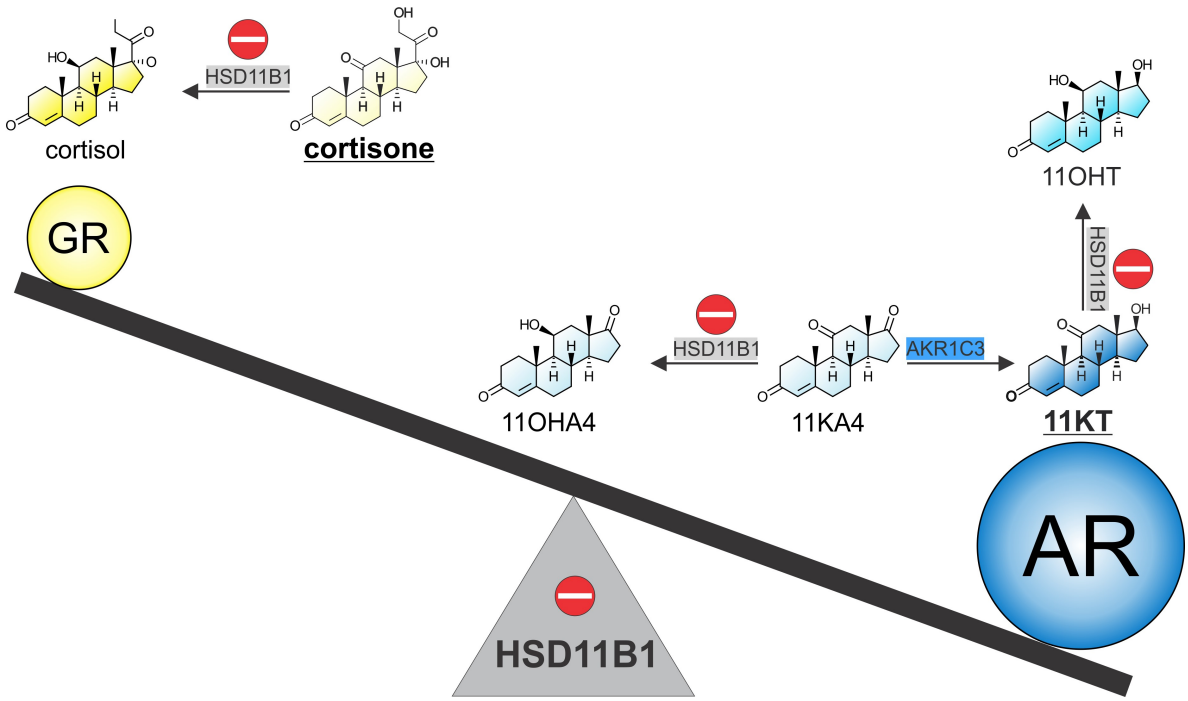

40

41 **Introduction**

42 The 11-oxygenated androgens are a group of adrenal-derived and peripherally activated androgens
43 that make a significant contribution to the circulating androgen pool, particularly in women (1–4). The
44 most potent 11-oxygenated androgen in circulation is 11-ketotestosterone (11KT), which has been
45 shown to bind to and activate the androgen receptor with an affinity and potency similar to
46 testosterone (5). Moreover, several studies have also shown that 11KT circulates at concentrations
47 equal to or higher than those of testosterone in women (3, 6, 7). Unlike the classic androgens, 11-
48 oxygenated androgens do not decline with age, with the result that 11KT is the most abundant active
49 androgen in the circulation of postmenopausal women (3, 6). While the role of 11-oxygenated
50 androgens in healthy individuals has yet to be defined, these androgens have been shown to play a
51 role in disease states such as polycystic ovary syndrome (PCOS), congenital adrenal hyperplasia (CAH),
52 Cushing's syndrome and castration resistant prostate cancer (CRPC) (8–12).

53 The biosynthesis of 11KT begins in the adrenal, where cytochrome P450 11B1 (CYP11B1) catalyses the
54 11β-hydroxylation of locally produced androstenedione to yield 11β-hydroxyandrostenedione
55 (11OHA4). 11OHA4 is released into circulation, and serves as the primary precursor for the
56 biosynthesis of 11KT by peripheral tissues (**Figure 1**). Specifically, 11OHA4 is converted to 11-
57 ketoandrostenedione (11KA4) by mineralocorticoid target tissues expressing 11β-hydroxysteroid
58 dehydrogenase type 2 (HSD11B2), such as the kidney (13). 11KA4 then subsequently serves as the
59 substrate for the key androgen activating enzyme, aldo-keto reductase 1C3 (AKR1C3), which is
60 abundantly expressed in adipose tissue (14–17). Notably, AKR1C3 catalyses the conversion of 11KA4
61 to 11KT significantly more efficiently than that of androstenedione to testosterone (16, 17). The
62 biosynthesis of 11KT is, however, more complex than that of testosterone as the presence of the 11-
63 keto group makes both 11KA4 and 11KT substrates for 11β-hydroxysteroid dehydrogenase type 1
64 (HSD11B1)—an enzyme best known for amplification of glucocorticoid signalling, which it achieves by
65 converting the inactive cortisone to active cortisol in key metabolic tissues including the liver, adipose
66 tissue and skeletal muscle (11, 18–20). Given that AKR1C3 and HSD11B1 are co-expressed in adipose
67 tissue, we propose that HSD11B1 regulates the amount of 11KT produced in two ways. First, by

68 competing with AKR1C3 for 11KA4, thereby limiting the amount of 11KA4 converted to 11KT by
69 AKR1C3. Secondly, by converting some of the 11KT formed to the far less androgenic 11β-
70 hydroxytestosterone (11OHT) (11) (**Figure 1**).

71 This proposed mechanism is important when considering that HSD11B1 has long been a therapeutic
72 target for prevention of tissue-specific excess glucocorticoid exposure and treatment of related
73 adverse metabolic effects (19, 21–24). Promising preclinical studies in rodents, which crucially do not
74 produce 11-oxygenated androgens (25–30), were unable to accurately model competing HSD11B1 and
75 AKR1C3 effects in humans. Our proposed hypothesis could provide an explanation for the more limited
76 effect sizes observed in clinical trials with HSD11B1 inhibitors (31, 32, 41, 42, 33–40), as increased 11KT
77 production resulting from HSD11B1 inhibition could counteract beneficial effects of reduced
78 glucocorticoid signalling, by increasing androgen signalling. This is particularly significant in women
79 where elevated androgens are linked to insulin resistance, type 2 diabetes, hypertension,
80 cardiovascular disease and non-alcoholic fatty liver disease (NAFLD), in particular in the context of
81 polycystic ovary syndrome, for which androgen excess is a defining feature (43–52).
82 Here, we characterised the interplay between HSD11B1 and AKR1C3 as co-regulators of 11KT
83 biosynthesis using a combination of *in vitro*, *in silico*, and human *ex vivo* and *in vivo* approaches
84 including selective HSD11B1 inhibitor treatment in individuals with type 2 diabetes.

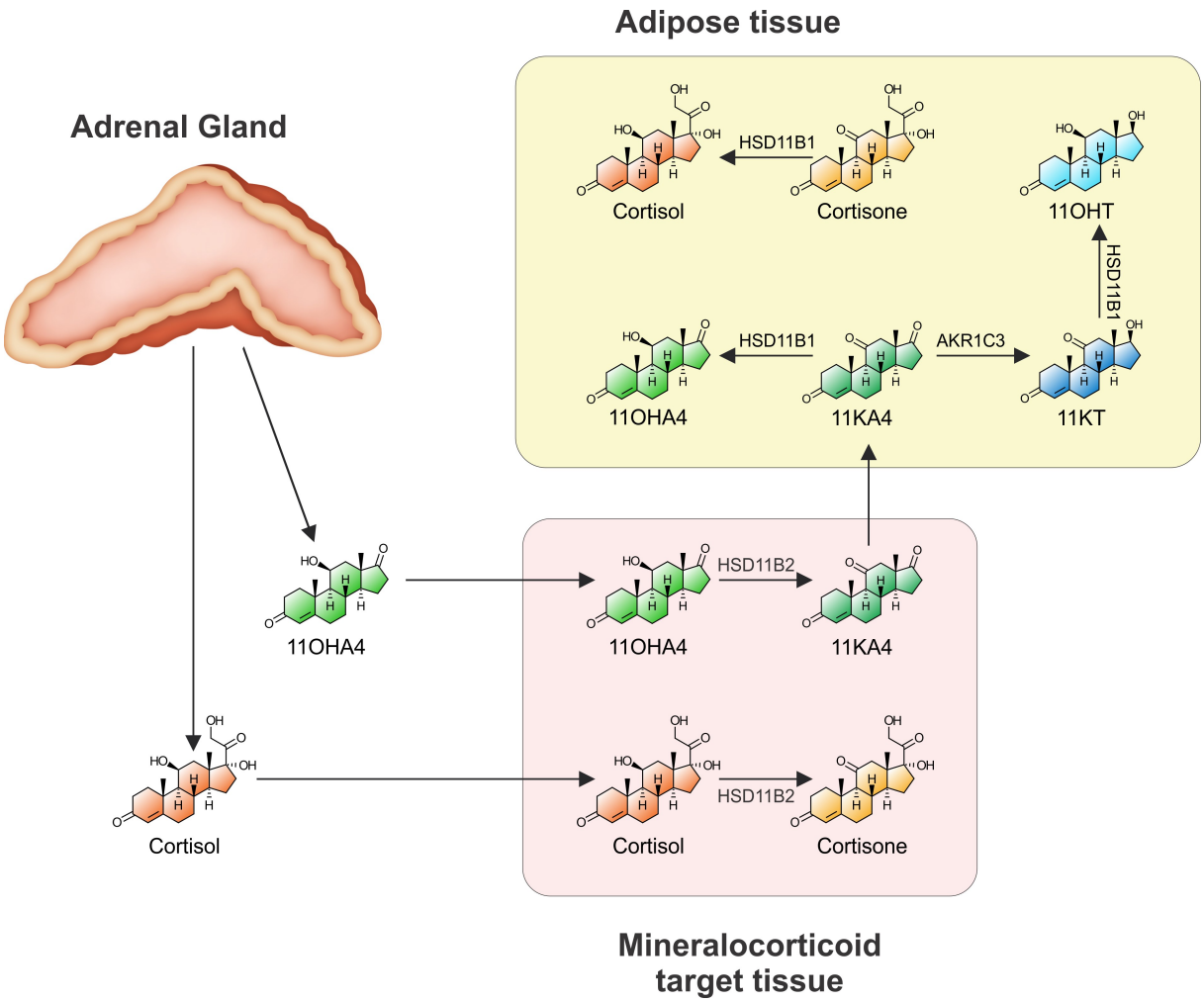

Figure 1: Schematic showing the peripheral metabolism of cortisol and 11OHA4. Cortisol is converted to its inactive form, cortisone, by HSD11B2 expressed in mineralocorticoid target tissues. Cortisone is in turn converted back to cortisol by HSD11B1 expressed in glucocorticoid target tissues (e.g., adipose). Like cortisol, adrenal derived 11OHA4 is a substrate for HSD11B2, yielding 11KA4. 11KA4 is a substrate for both the androgen activating enzyme AKR1C3 and HSD11B1, both of which are expressed in adipose tissue. Conversion of 11KA4 to 11OHA4 by HSD11B1 prevents the conversion of 11KA4 to the potent 11-oxygenated androgen, 11KT. The 11KT that is produced by AKR1C3 is also a substrate for HSD11B1, yielding the substantially less active androgen, 11OHT.

Results

HSD11B1 efficiently catalyses the 11β-reduction of 11-oxygenated androgens.

Non-steroidogenic HEK293 cells were transiently transfected to express HSD11B1 and activity assayed. Rate equations were fitted to the progress curves for three independent experiments as shown in **Supplementary Figure 1**. A low but detectable reverse reaction rate was observed for the cortisone to cortisol and the 11KA4 to 11OHA4 reactions. Reversible kinetics were therefore used for these reactions. Our results show that the apparent K_m ($K_{m,\ app}$) of HSD11B1 for cortisone and 11KA4 are similar (0.9 µM and 1 µM), while the $K_{m,\ app}$ for 11KT (0.21 µM) is >4-fold lower, indicating a higher affinity towards 11KT (**Table 1**). However, the apparent V_{max} ($V_{max,\ app}$) for 11KT (0.05 µM/h) was >2-fold lower than that for cortisone (0.12 µM/h) and 7-fold lower than that for 11KA4 (0.35 µM/h). Considering the V_{max}/K_m values, an estimate of enzyme efficiency, both 11KA4 and 11KT are more efficiently converted to their respective products than the traditionally recognised HSD11B1 substrate cortisone.

Table 1: Kinetic constants ($K_{m,\ app}$; $V_{max,\ app}$; V_{max}/K_m) determined for HSD11B1.

Reaction	$K_{m,\ app\ (substrate)}$ (µM)	$K_{m,\ app\ (product)}$ (µM)	$V_{max,\ app\ (forward)}$ (µM/h)*	$V_{max,\ app\ (reverse)}$ 1/h[a] or (µM/h)[b]	V_{max}/K_m#
Cortisone -> Cortisol	0.9	-	0.12	0.01[a]	0.13
11KA4 -> 11OHA4	1	2.46	0.35	0.03[b]	0.35
11KT -> 11OHT	0.21	-	0.05	-	0.24

*$V_{max,\ app}$ values are dependent on transfection efficiency and differ between experiments. We included the conversion of 100 nM 11KA4 to 11OHA4 in all experiments and used the initial rate to normalise the transfection efficiency, which was set to 1 for the values reported above.
#V_{max}/K_m values are reported for the substrate and forward reaction.

Co-expression of HSD11B1 with AKR1C3 modulates the activation of 11-oxygenated androgens.

AKR1C3 is the key enzyme catalysing the peripheral conversion of androgen precursors into active androgens (14). We have previously shown that AKR1C3 catalyses the conversion of 11KA4 to the potent androgen 11KT 8-fold more efficiently than the conversion of androstenedione to testosterone

118 (16). To determine how the co-expression of HSD11B1 with AKR1C3 would affect 11KT production, we
119 mixed transfected HEK293 cells expressing either AKR1C3 or HSD11B1 to obtain increasing ratios of
120 HSD11B1:AKR1C3, while keeping the number of cells expressing AKR1C3 constant. The total cell count
121 was also kept constant by including cells transfected with an empty plasmid as required. The relative
122 expression of HSD11B1:AKR1C3 was confirmed by qPCR (**Figure 2A**). Increased ratios of
123 HSD11B1:AKR1C3 resulted in increased concentrations of cortisol being produced upon addition of
124 100 nM cortisone (**Figure 2B**), thereby confirming the increased HSD11B1 expression. Similarly,
125 increasing the ratio of HSD11B1:AKR1C3 resulted in the concomitantly increased production of
126 11OHA4 from 11KA4, with 11OHA4 becoming the most abundant product when the HSD11B1:AKR1C3
127 ratio was increased beyond 0.1:1 (**Figure 2C**). Biosynthesis of 11KT was highest when AKR1C3 was
128 expressed in the absence of HSD11B1, with increasing HSD11B1:AKR1C3 ratios resulting in a rapid
129 decrease in the concentrations of 11KT. 11OHT initially increased as the ratio of HSD11B1:AKR1C3
130 increased, peaking at a ratio of 0.25:1. Further increases in the HSD11B1:AKR1C3 ratio resulted in
131 decreased concentrations of 11OHT being produced.

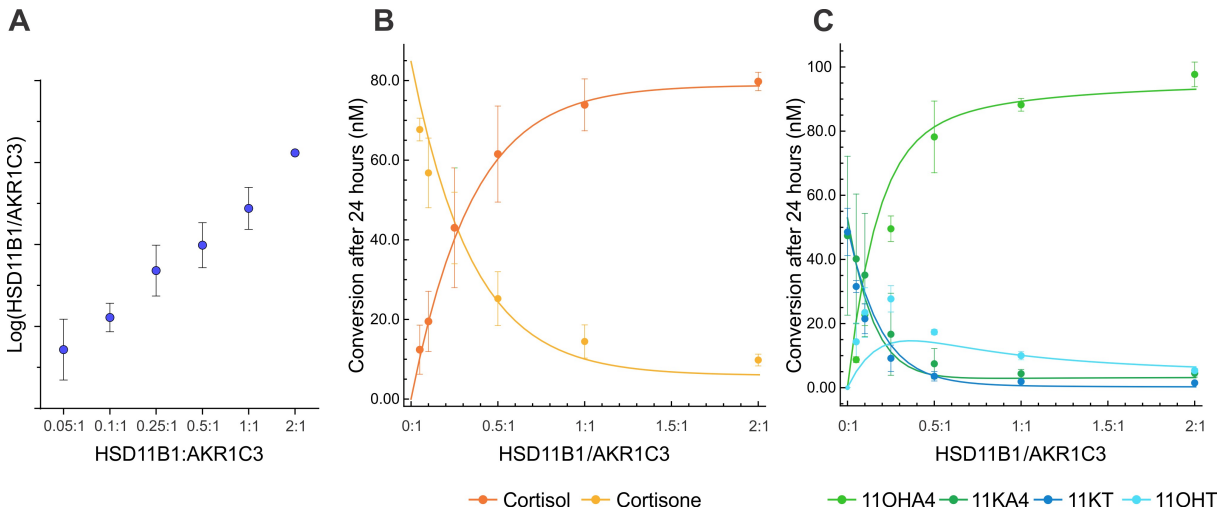

132

133 **Figure 2: Increased HSD11B1:AKR1C3 ratios modulate the biosynthesis of 11KT. (A)** qPCR data
134 confirming the increase in HSD11B1 expression relative to that of AKR1C3 at the different
135 HSD11B1:AKR1C3 ratios. **(B)** The conversion of cortisone (0.1 µM) to cortisol by increasing ratios of
136 HSD11B1:AKR1C3 after 24 hours **(C)**. The conversion of 11KA4 (0.1 µM) to 11OHA4, 11KT and 11OHT
137 by increasing ratios of HSD11B1:AKR1C3 after 24 hours. For **B** and **C** the experimental data from the
138 ratio experiments are shown as points with error bars, while the computational models' predictions
139 are shown with the solid connecting lines. All results are shown as means ± SEM of three independent
140 experiments.
141

142 Using the parameterised rate equations for HSD11B1 and those previously determined by us for
143 AKR1C3 (16), a computational model consisting of a set of ordinary differential equations was
144 constructed to simulate steroid metabolism in cells with both enzymes expressed:

145 $$\frac{d\,\mathrm{ka4}(t)}{d\,\mathrm{t}} = -v_{\mathrm{HSD_ka4}} - v_{\mathrm{AKR_ka4}};\ \frac{d\,\mathrm{oha4}(t)}{d\,\mathrm{t}} = v_{\mathrm{HSD_ka4}};\ \frac{d\,\mathrm{kt}(t)}{d\,\mathrm{t}} = v_{\mathrm{AKR_ka4}} - v_{\mathrm{HSD_kt}};\ \frac{d\,\mathrm{oht}(t)}{d\,\mathrm{t}} = v_{\mathrm{HSD_kt}}$$

146 The rate equations for HSD11B1 and AKR1C3 are given in the Supplementary material. The model was
147 able to predict the experimentally determined effect of increasing HSD11B1:AKR1C3 ratios on the
148 metabolism of cortisone and 11KA4, respectively (**Figure 2**). Note that the kinetic parameters in the
149 mathematical model were not fitted to the experimental data for the different HSD11B1:AKR1C3
150 ratios, but were determined in the progress curves for the individual incubations (**Supplementary**
151 **Figure 1)**. Taken together these data clearly show that HSD11B1 modulates the biosynthesis of 11KT
152 by AKR1C3, and that the model can predict the effect of varying HSD11B1:AKR1C3 ratios.

153

154 ***In vitro* inhibition of HSD11B1 results in the accumulation of 11-ketotestosterone.**

155 Next, we set out to determine the effect of HSD11B1 inhibition on 11KT biosynthesis. We mixed
156 HEK293 cells transiently transfected with either AKR1C3 or HSD11B1 at a ratio of 1:1 and
157 simultaneously treated the cells with cortisone and 11KA4 in the absence and presence of the HSD11B1
158 inhibitor, carbenoxolone (CBX). We used either equimolar concentrations of cortisone and 11KA4 (100
159 nM each) or 10-fold excess of cortisone (100 nM) over 11KA4 (10 nM) to more closely mimic circulating
160 concentrations (3). Our results show that CBX reduced the production of cortisol from cortisone from
161 56.5 nM to 3.2 nM after 24 hours, demonstrating effective HSD11B1 inhibition (**Figure 3A & B**). In the
162 absence of CBX the majority of 11KA4 (69%) was converted to 11OHA4 by HSD11B1, with only 3.8 nM
163 of 11KT produced from 100 nM 11KA4 by AKR1C3 (**Figure 3C**). However, inhibition of HSD11B1 resulted
164 in a 7-fold increase in 11KT production after 24 hours (**Figure 3D**). Similarly, in cells treated with 100
165 nM cortisone and 10 nM 11KA4, inhibition of HSD11B1 by CBX resulted in a 12-fold increase in 11KT
166 production (0.15 nM without CBX to 1.8 nM with CBX) (**Figure 3E & F**). 11KT was the by far most
167 abundant 11-oxygenated androgen following inhibition of HSD11B1. Inhibition of both the conversions
168 from 11KA4 to 11OHA4 and 11KT to 11OHT, respectively, allowed AKR1C3 to catalyse the conversion

169 of 11KA4 to 11KT without the need to compete for substrate and prevented the inactivation of 11KT

170 to the less potent 11OHT. The computational model was able to independently predict the outcome

171 of HSD11B1 inhibition under the experimental conditions (**Figure 3**).

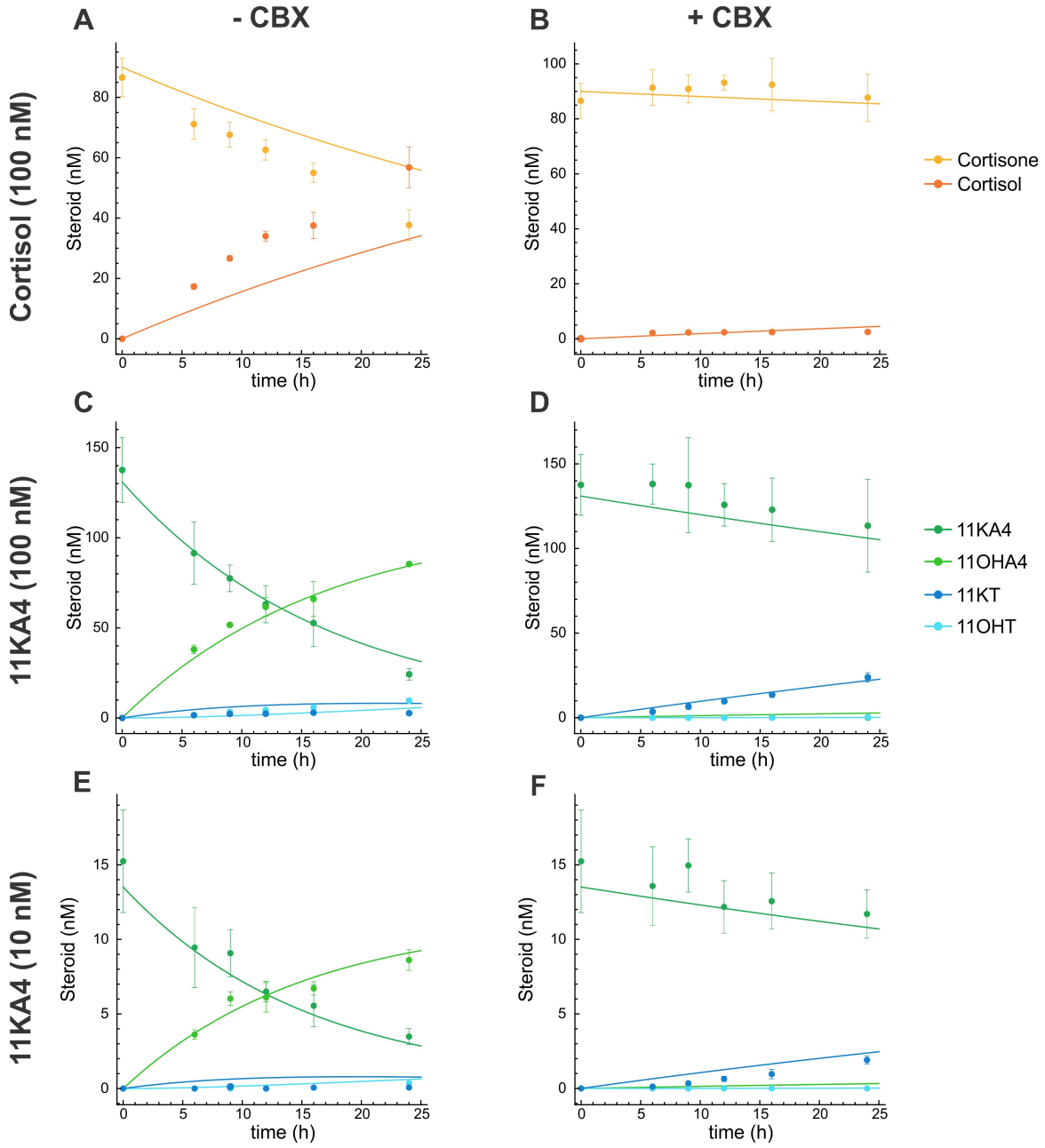

172

173 **Figure 3: Inhibition of HSD11B1 by carbenoxolone (CBX) inhibits the biosynthesis of cortisol, but**
174 **allows for increased AKR1C3-mediated production of 11KT when HSD11B1 and AKR1C3 are co-**
175 **expressed.** HEK293 cells expressing HSD11B1 and AKR1C3 were combined at a ratio of 1:1 and treated
176 with either 100 nM cortisone **(A & B)** and 100 nM 11KA4 **(C & D)** with and without CBX (10 µM) or 100
177 nM cortisone and 10 nM 11KA4 **(E & F)** with or without CBX (10 µM). The experimental data from the
178 time course experiment is shown as points with error bars, while the computational models'
179 predictions are shown with the solid lines. All results are shown as means ± SD of a single biological
180 experiment performed in triplicate. This enabled the model to predict the outcomes from one
181 experiment with the same transfection efficiency.
182

183 ***In silico* analysis of the combined effect of HSD11B1:AKR1C3 co-expression and HSD11B1 inhibition**
184 **on 11KT biosynthesis.**

185 After having shown that the computational model was able to individually predict both the effect of
186 increasing HSD11B1:AKR1C3 ratios (**Figure 2**) and the effect of HSD11B1 inhibition (**Figure 3**), we used
187 the model to simultaneously predict the effect of differing HSD11B1 and AKR1C3 expression and
188 differing degrees of HSD11B1 inhibition on the conversion of 10 nM 11KA4 to 11OHA4, 11KT and
189 11OHT after 24 hours (**Figure 4**). These results confirmed that HSD11B1 strongly modulates the
190 biosynthesis of 11KT by competing for the precursor, 11KA4, and by converting the 11KT that is formed
191 to the less potent androgen 11OHT. The inhibition of HSD11B1 reduced these effects under all
192 HSD11B1:AKR1C3 ratios tested leading to increased production of 11KT. Notably, lower ratios of
193 HSD11B1:AKR1C3 were more sensitive to HSD11B1 inhibition, more quickly leading to increased 11KT
194 concentrations as the level of inhibition was increased. Higher absolute concentrations of 11KT were
195 also produced by lower ratios of HSD11B1:AKR1C3 (AKR1C3 was kept constant) when HSD11B1 was
196 inhibited up to the maximum simulated I/Ki value of ten. Near complete inhibition of HSD11B1 (I/Ki =
197 100), however, negated the effect of the HSD11B1:AKR1C3 ratio with 11KT production dependent only
198 on AKR1C3 (**Supplementary Figure 2**). The effect of HSD11B1 inhibition is therefore dependent on the
199 degree of inhibition, the ratio of HSD11B1:AKR1C3 and the absolute expression level of HSD11B1 and
200 AKR1C3

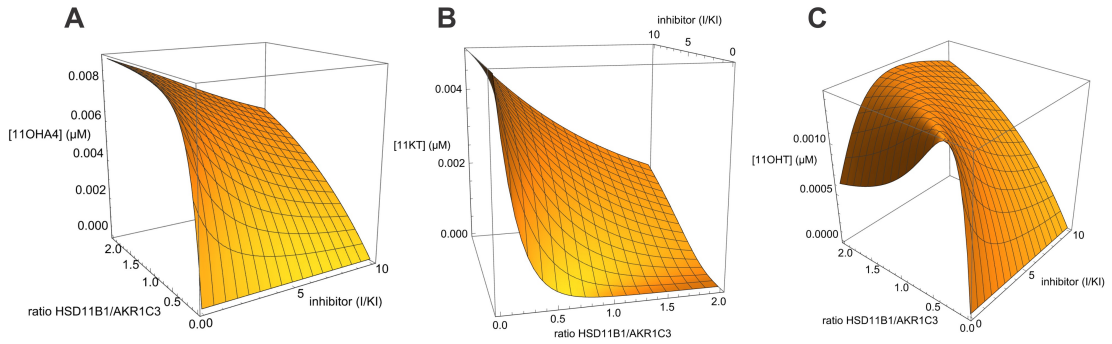

201

202 **Figure 4: Computational model of the effect of varying HSD11B1:AKR1C3 ratios and different levels**
203 **of HSD11B1 inhibition on the resulting concentrations of 11OHA4 (A), 11KT (B) and 11OHT (C).** The
204 model varies that ratio of HSD11B1:AKR1C3 as in Figure 2 and estimates the effect of different levels
205 of HSD11B1 inhibition on the conversion of 10 nM 11KA4 after 24 hours as in Figures 2 and 3.

206 ***In vitro* inhibition of HSD11B1 increases androgen receptor activation.**

207 To investigate the potential biological impact of HSD11B1 inhibition, we combined HEK293 cells
208 expressing AKR1C3 or HSD11B1 at a 1:1 ratio and incubated the cells with 100 nM cortisone and 10
209 nM 11KA4 in the absence and presence of CBX for 24 hours. The conditioned media were then
210 transferred to HEK293 cells transiently transfected with either a plasmid expressing the glucocorticoid
211 receptor (GR) or the androgen receptor (AR), and a luciferase reporter construct. The GR- and AR-
212 mediated induction of luciferase was subsequently measured after an additional 24 hour incubation.
213 As expected, HSD11B1 mediated the conversion of cortisone to cortisol, with the resulting cortisol
214 increasing the transactivation of the GR (94-fold induction). Inhibition of HSD11B1 with CBX reduced
215 cortisol production 32-fold (**Figure 5A**) and resulted in a 34-fold decrease in GR transactivation (**Figure**
216 **5B**). Conversely, inhibition of HSD11B1 resulted in a 7-fold increase in transactivation of the AR due to
217 significantly increased 11KT biosynthesis (**Figure 5C & D**). Basal levels of AR transactivation in the
218 absence of CBX and 11KT were due to the presence of low concentrations of 11OHT (0.81 nM;
219 **Supplementary Figure 3**), which is a partial agonist of the AR (11, 53). It should be noted that we
220 observed that CBX weakly antagonises the AR (**Supplementary Figure 4**), hence, the induction of the
221 AR was likely underestimated. Nonetheless, taken together, these data demonstrate that while
222 inhibition of HSD11B1 results in the desired decrease in GR transactivation, this is accompanied by a
223 shift towards AR transactivation.

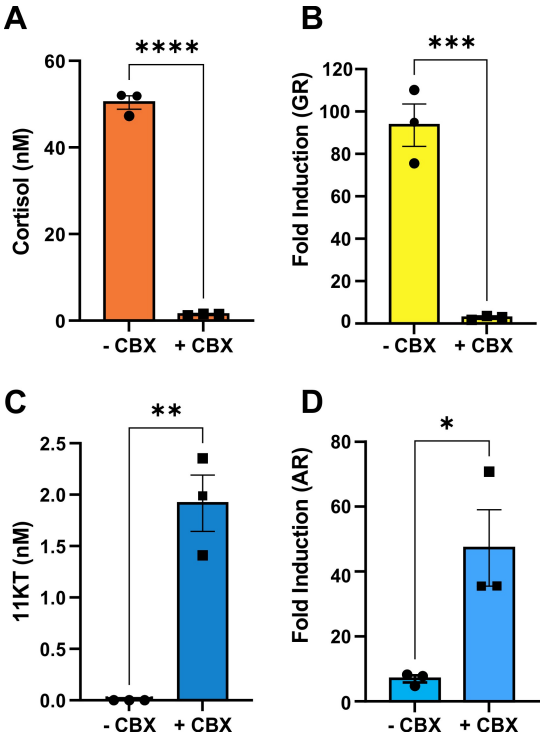

Figure 5: Inhibition of HSD11B1 by carbenoxolone (CBX) results in decreased cortisol production (A) and an accompanying decrease in transactivation of the glucocorticoid receptor (B), but increased production of 11KT (C) and transactivation of the androgen receptor (D). HEK293 cells expressing HSD11B1 and AKR1C3 were combined at a ratio of 1:1 and treated with 100 nM cortisone and 10 nM 11KA4 with or without CBX (10 µM). After 24 hours the conditioned media was transferred to HEK293 cells transiently transfected with either a plasmid expressing the glucocorticoid receptor (GR) and a luciferase reporter construct or a plasmid expressing the androgen receptor (AR) and the same luciferase reporter construct. Luciferase was assayed after an additional 24 hour incubation and is shown as the fold-induction relative to a vehicle control. All results are shown as means ± SEM of three biological experiments. P values were calculated using unpaired t-tests (*P <0.05; **P<0.01; ***P<0.001; ****P <0.0001)**.**

Selective HSD11B1 inhibition increases 11KT production in female human adipose tissue *ex vivo*.

We next set out to determine the effect of HSD11B1 inhibition on 11KT biosynthesis in paired subcutaneous and omental adipose tissue samples from women undergoing elective bariatric surgery. For these experiments we employed the selective HSD11B1 inhibitor AZD4017 (54). The conversion of cortisone to cortisol was reduced to 3% of the uninhibited conversion rate in subcutaneous adipose tissue treated with AZD4017, thereby confirming effective HSD11B1 inhibition (**Figure 6A**). Following incubation of subcutaneous adipose tissue with 11KA4 (100 nM), the most abundant product formed in the absence of AZD4017 was 11OHT (60.1% of total products formed), followed by 11OHA4 (23.4%) and 11KT (16.5%) (**Figure 6F**). The biosynthesis of both 11KT and 11OHT is dependent on AKR1C3 activity and the observed sum of 11KT and 11OHT (76.6% of products formed) suggested substantial

247 AKR1C3 expression. This was confirmed by qPCR analysis, which showed higher AKR1C3 expression
248 relative to that of HSD11B1 (**Figure 6C**). However, HSD11B1 converted 78.5% of the 11KT formed to
249 the less active 11OHT. Inhibition of HSD11B1 by AZD4017, resulted in a 5-fold increase in 11KT, with
250 11KT becoming the most abundant product (85.6%) (**Figure 6G**). This was accompanied by significant
251 decreases in the production of both 11OHA4 and 11OHT (21-fold and 4.5-fold, respectively).
252 Marginally lower conversion of cortisone to cortisol was observed in omental adipose tissue as
253 compared to subcutaneous tissue, with AZD4017 again effectively inhibiting HSD11B1 activity (**Figure**
254 **6B**). Treatment with AZD4017 again resulted in a significant decrease in 11OHA4 and 11OHT
255 concentrations, with an accompanying 4-fold increase in 11KT production (**Figure 6H & I**).
256 The sum of 11KT and 11OHT (66.0%) was lower in the omental tissue than in subcutaneous tissue
257 (76.6%) illustrating lower AKR1C3 expression as confirmed by qPCR (**Figure 6C & D**). The ratio of
258 HSD11B1 over AKR1C3 expression was lower in subcutaneous than omental adipose tissue (**Figure 6E**),
259 favouring androgen activation in subcutaneous tissue vs glucocorticoid activation in omental tissue.
260 The metabolism of 11KA4 and the effect of AZD4017 inhibition in human adipose tissue was simulated
261 with the mathematical model that was constructed using conversion data obtained from transfected
262 HEK293 cells. The expression levels of the HSD11B1 and AKR1C3 in the adipose tissue relative to that
263 in transfected HEK293 cells therefore needed to be estimated. This was achieved by fitting the
264 expression levels of HSD11B1 to the cortisone to cortisol conversion data (**Figure 6A & B**) and then
265 using an AKR1C3 activity based on the AKR1C3/HSD11B1 expression ratio as determined by qPCR
266 (**Figure 6C & D**). This allowed the model to predict the conversion of 11KA4 to the respective products
267 over time. These simulation revealed the initial accumulation of 11KT, prior to the time dependent
268 conversion of this product to 11OHT by HSD11B1 (**Figure 6F &H**). Inhibition of HSD11B1 eliminated the
269 latter conversion yielding only 11KT and illustrated that the amount of 11KT formed over time was
270 dependent on the absolute expression levels of AKR1C3.
271 Taken together, these data indicate that inhibition of HSD11B1 in adipose tissue leads to a shift in the
272 metabolism of 11-oxygenated androgens resulting in increased 11KT biosynthesis.

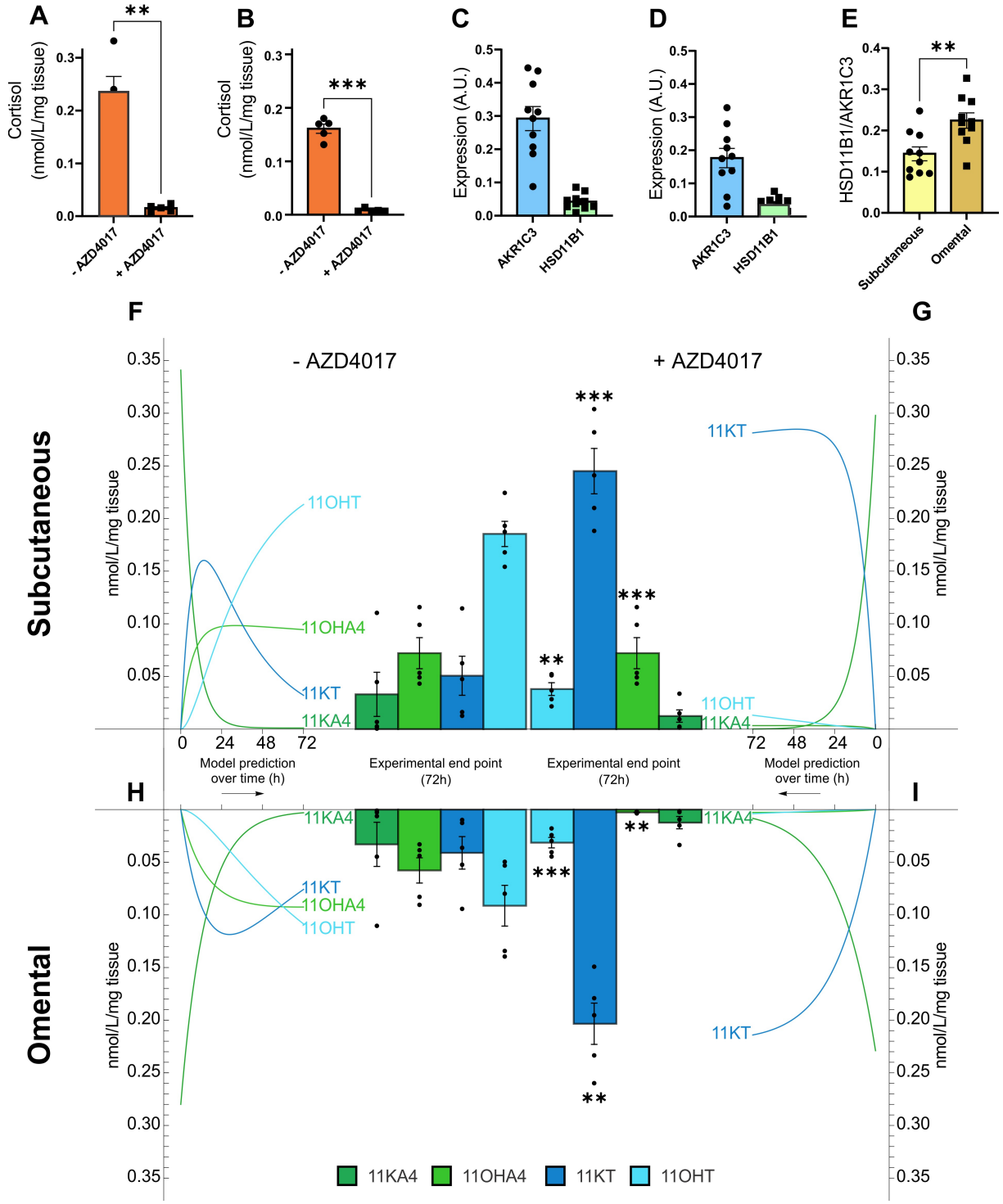

Figure 6: Inhibition of HSD11B1 by AZD4017 in human subcutaneous (A, F, G) and omental (B, H, I) adipose tissue results in the increased production of 11KT. Adipose tissue was incubated *ex vivo* with 100 nM cortisone (**A, B**) or 11KA4 (**F-I**) with or without AZD4017 (100 nM) for 72 hours. The mathematical model's prediction of the conversion over time is shown next to the experimentally determined end point data after the 72 hour incubation. Expression of AKR1C3 and HSD11B1 in subcutaneous (**C**) and omental (**D**) adipose tissue was measured by qPCR. The expression ratio of HSD11B1:AKR1C3 were determined for both adipose tissue subtypes (**E**). P values were calculated using Wilcoxon signed-rank tests (*P <0.05; **P<0.01; ***P<0.001).

284 ***In vivo* treatment with a selective HSD11B1 inhibitor increases circulating 11KT concentrations.**

285 After having shown that inhibition of HSD11B1 in adipose tissue shifts the metabolism of 11-
286 oxygenated androgens towards 11KT biosynthesis, we next set out to determine if inhibition of
287 HSD11B1 would alter circulating concentrations of 11KT. We therefore measured a panel of 11-
288 oxygenated androgens as well as cortisol and cortisone in the serum of individuals with type 2 diabetes
289 who had received treatment with the selective HSD11B1 inhibitor AZD4017 during a randomized,
290 double-blind, parallel-group, placebo-controlled phase 2b pilot trial (40). Paired (day 0 and day 35)
291 samples were available for 18 participants (13 men and 5 women; median BMI 32.2 kg/m^2 range 25.0-
292 47.5 kg/m^2; median age 64.5, range 28-84 years), with 11 randomised to HSD11B1 inhibitor treatment
293 (7 men and 4 women) and 7 (6 men and 1 woman) to placebo.

294 Our measurements confirmed that AZD4017 significantly reduced the serum cortisol/cortisone ratio,
295 indicating effective HSD11B1 inhibition as previously reported for selected urinary glucocorticoid
296 metabolites by LC-MS/MS (40), and further confirmed here by GC-MS **(Supplementary Figure 5)**.
297 However, concomitantly, circulating 11KT concentrations significantly increased 2.5-fold (from 1.7 to
298 4.3 nM) following treatment with 400 mg AZD4017 twice daily for 35 days. This was accompanied by
299 a significant, 2-fold decrease in 11OHT concentrations and a 4-fold decrease in the 11OHT/11KT ratio
300 **(Figure 7)**. While the circulating concentrations of the 11-oxygenated androgen precursors 11OHA4
301 and 11KA4 did not change, a small, but significant decrease was also observed for the 11OHA4/11KA4
302 ratio. These changes were also reflected by a significant increase in the urinary metabolite 11-
303 oxoandrosterone, which is derived from 11KA4 and 11KT (55), and a 6-fold decrease in the 11β-
304 hydroxyandrosterone/11-oxoandrosterone ratio **(Figure 7)**. No changes in the serum concentrations
305 of 11-oxygenated androgens were observed in the placebo-treated group (**Supplementary Figure 6**).

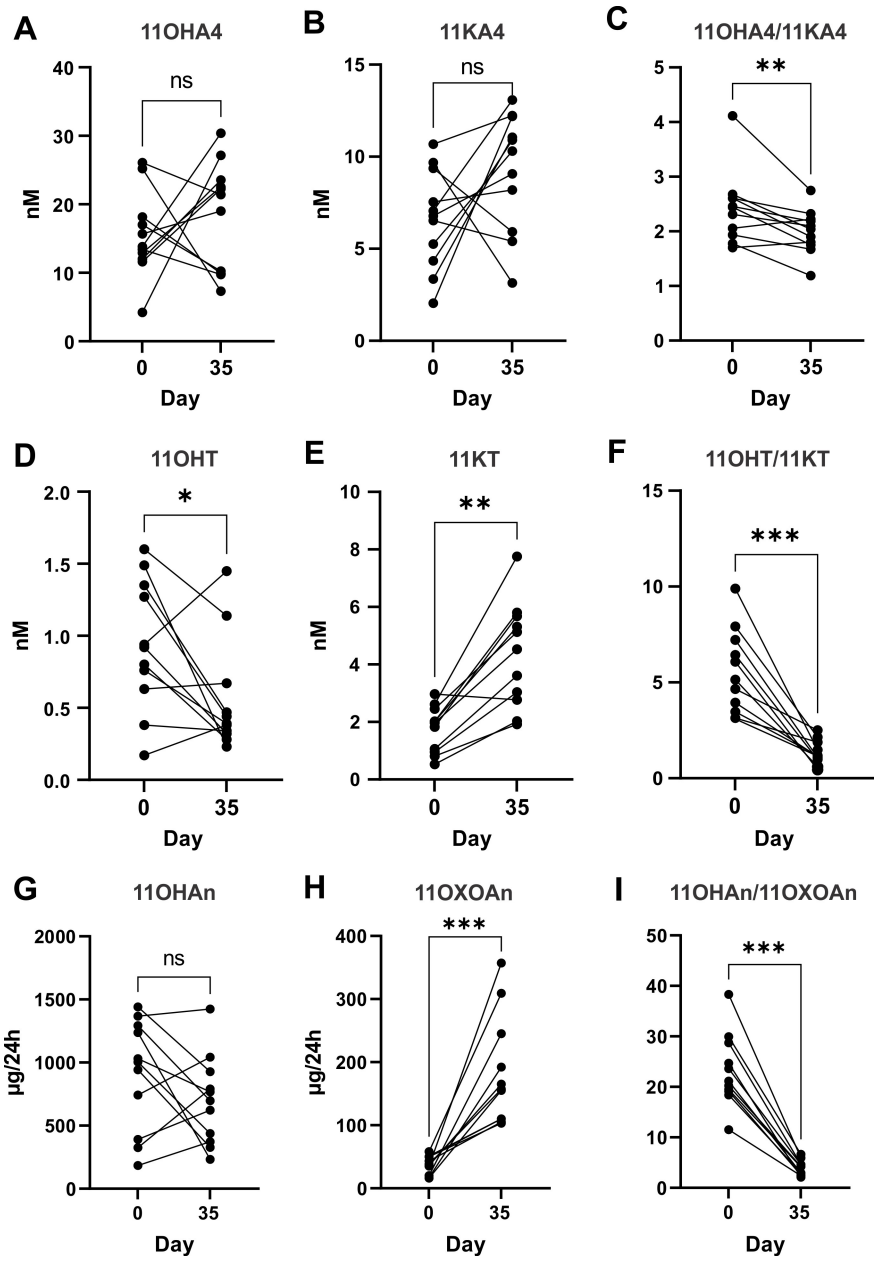

Figure 7: Inhibition of HSD11B1 by oral administration of AZD4017 (400 mg twice daily) for 35 days (n=11) changes the serum (A-F) and urinary (G-I) profile of 11-oxygenated androgens and their metabolites, with significant increases in the circulating concentration of the potent androgen 11KT. P values were calculated using Wilcoxon signed-rank tests (*P <0.05; **P<0.01; ***P<0.001). Serum concentrations of classic androgens are shown in **Supplementary Figure 7**.

When considering correlations between the changes in circulating steroid concentrations, it is interesting to note that the cortisol/cortisone ratio is highly correlated with the change in both the ratios of 11OHA4/11KA4 (R = 0.893; P < 0.001) and 11OHT/11KT (R = 0.686; P < 0.01), but not with the change in circulating 11KT (R = -0.375; P = 0.126) (**Supplementary Table 1**).

319 **Discussion**

320 The relatively recent identification of 11-oxygenated androgens as important contributors to the
321 human androgen pool has prompted a re-evaluation of existing paradigms. One such paradigm is the
322 idea that the two HSD11B isoforms are predominantly involved in the peripheral metabolism of
323 glucocorticoids. We and others have previously shown that HSD11B1 and HSD11B2 are essential for
324 the interconversion of the 11β-hydroxyl and 11-keto forms of the 11-oxygenated androgens (11, 20).
325 We have also previously shown that 11KA4, but not 11OHA4, is a substrate for the key androgen-
326 activating enzyme AKR1C3 (16, 17). Therefore, HSD11B2 plays a vital role in catalysing the conversion
327 of adrenal-derived 11OHA4 to 11KA4, which can then be converted to the potent androgen 11KT by
328 AKR1C3 (13). One of the main sites of AKR1C3 expression and peripheral androgen activation is adipose
329 tissue (14, 15) which also abundantly expresses HSD11B1 (18, 19, 22). Here, using a combination of *in*
330 *vitro*, *in silico* and *ex vivo* studies, we demonstrate that co-expression of HSD11B1 with AKR1C3
331 modulates peripheral biosynthesis of 11KT, first, by competing with AKR1C3 for the substrate 11KA4,
332 and, second, by converting much of the resulting 11KT to the less potent androgen 11OHT. We
333 demonstrated that inhibition of HSD11B1 results in significantly increased 11KT biosynthesis as shown
334 by us *in vitro*, *in silico*, *ex vivo* and in a phase 2a study comparing the effects of 35 days of treatment
335 with the selective HSD11B1 inhibitor AZD4017 to placebo treatment. Our data show that HSD11B1
336 inhibition does not only alter local, adipose tissue-specific 11KT concentrations, but also systemic
337 levels, thus emphasising that peripheral tissues expressing AKR1C3 are essential for 11KT biosynthesis
338 (13). Collectively, our findings show that under normal circumstances HSD11B1 plays an important
339 novel role in preventing 11KT accumulation, in addition to its well-known role in local glucocorticoid
340 activation.

341 Our findings are of immediate clinical relevance, particularly in women, where circulating
342 concentrations of 11KT are similar to testosterone concentrations (3, 6, 56, 57). Therefore, increasing
343 11KT due to HSD11B1 inhibition markedly increases the total circulating pool of active androgens in
344 women. This increase in androgen load is significant given that 11KT has shown functional activity
345 comparable to testosterone (5, 53, 58) and increased circulating androgens have been linked to a

346 significantly greater risk of type 2 diabetes in women (43). Moreover, there is growing evidence that
347 androgens drive the risk of common metabolic disorders, including type 2 diabetes, hypertension,
348 cardiovascular disease and NAFLD (15, 43, 59–62, 44, 46–52), in women with PCOS where androgen
349 excess is a hallmark (62). Our finding of increased 11KT biosynthesis to clinically highly relevant
350 concentrations occurring after HSD11B1 inhibition needs to be taken into account when considering
351 HSD11B1 inhibition as treatment for type 2 diabetes or metabolic syndrome in women, as the
352 beneficial effects of reduced local glucocorticoid activation could be offset by opposing metabolic
353 effects due to increased 11KT concentrations and AR signalling. This is highly relevant for the recently
354 proposed use of HSD11B1 inhibitors in ameliorating the metabolically adverse consequences of mild
355 autonomous cortisol excess (MACS) due to adrenal adenomas (63) as affected patients are
356 predominantly female (64).
357 Notably, quantification of AKR1C3 and HSD11B1 expression levels in subcutaneous and omental
358 adipose tissue revealed a degree of interpersonal variation. Our computational simulations revealed
359 that variations in the relative, as well as the absolute expression levels of HSD11B1 and AKR1C3 would
360 result in individual differences in the amount of 11KT produced as well as the magnitude of change
361 upon HSD11B1 inhibition. Indeed, this biological variation was reflected in both the *ex vivo* adipose
362 tissue conversion data and the serum concentrations of 11KT before and after administration of
363 AZD4017 in individuals with type 2 diabetes. Our simulations suggest that when considering 11KT
364 biosynthesis, individuals with higher HSD11B1 expression relative to AKR1C3 would be less responsive
365 to partial HSD11B1 inhibition. However, if HSD11B1 activity is completely abolished by inhibition then
366 the amount of 11KT produced is dependent of the absolute levels of AKR1C3 expressed. Increased
367 11KT concentrations are therefore not solely dependent on the inhibition of HSD11B1, but also on the
368 amount of AKR1C3 expressed. Notably, AKR1C3 expression correlates with BMI in subcutaneous, but
369 not omental, adipose tissue and its expression is upregulated by insulin (14, 15, 17). Women with
370 insulin resistance and obesity due to metabolic syndrome are therefore likely to have high expression
371 levels of AKR1C3 (14, 15), which would result in greater increases in 11KT upon inhibition of HSD11B1.
372 Thus, while such women may benefit from the local reduction of glucocorticoid activation by HSD11B1

373 inhibition in adipose tissue, they may be primed to generate more 11KT. Indeed, we noted that the
374 expression of AKR1C3 was higher than that of HSD11B1 in adipose tissue obtained from women with
375 obesity undergoing elective bariatric surgery. As a result, the conversion of 11KA4 yielded more 11KT
376 and 11OHT combined (both requiring AKR1C3 activity) than 11OHA4. In subcutaneous adipose tissue,
377 which had a lower HSD11B1:AKR1C3 ratio compared to omental adipose tissue, 11OHT was the most
378 abundant product, demonstrating effective conversion of 11KA4 to 11KT by AKR1C3 and subsequent
379 conversion of 11KT to 11OHT by HSD11B1. Similarly, we noted that in our clinical cohort, which
380 consisted of individuals with type 2 diabetes (BMI mostly in the obese range), the mean circulating
381 11OHT concentration was ≥2-fold higher than previously reported for healthy individuals thus
382 suggesting high peripheral AKR1C3 expression (3). Interestingly, a previous *ex vivo* study found that
383 androgen exposure upregulates HSD11B1 expression in adipose tissue (65) emphasising that
384 inactivation of 11-oxygenated androgens by HSD11B1 might be a protective mechanism, that no longer
385 suffices once AKR1C3 is significantly upregulated, e.g. in the context of PCOS (15).
386 Increased 11KT concentrations following HSD11B1 inhibition are unlikely to be a concern in men as the
387 metabolic effects of androgens are sexually dimorphic. In men, reduced androgen concentrations are
388 associated with adverse metabolic consequences, including insulin resistance, type 2 diabetes and
389 metabolic syndrome, and as such increased 11KT levels have the potential to be beneficial (43, 61,
390 66). Glucocorticoids are, however, also known to have sexually dimorphic effects, which are further
391 complicated by crosstalk between glucocorticoids and androgens (67–69). Unfortunately, the vast
392 majority of HSD11B1 inhibitor clinical studies did not report sex-specific outcomes for HSD11B1
393 inhibition (34–38). Larger sex-specific studies are therefore needed to fully assess the benefits of
394 HSD11B1 inhibition in relation to metabolic conditions, while taking into account potential opposing
395 androgenic effects in women, resulting from increased 11KT.
396 One recent study by Hardy *et al.* investigated the effects of HSD11B1 inhibition in women with obesity
397 and Idiopathic Intracranial Hypertension (41). Twice daily administration of 400 mg AZD4017 for 12
398 weeks had no effect on fasting glucose, fasting insulin, insulin resistance or HbA1c, in agreement with
399 our hypothesis that androgenic effects may counter beneficial metabolic effects of reduced

400 glucocorticoid concentrations. Furthermore, this study found no effect of HSD11B1 inhibition on
401 adipose or bone composition, but did report reduced cholesterol and increased HDL with HSD11B1
402 inhibition suggesting that women do exhibit some cardioprotective responses to HSD11B1 inhibition.
403 Importantly, Hardy *et al*. also reported increased lean muscle mass with HSD11B1 inhibition, which
404 correlated with increased testosterone and 11-oxygenated androgen precursors (11OHA4 and 11KA4)
405 levels; however, they did not report 11KT concentrations.
406 Increased adrenal output of 11OHA4 is not unexpected with HSD11B1 inhibition, which leads to
407 reduced negative feedback on the HPA-axis, increased ACTH levels and increased adrenal output of
408 cortisol and adrenal androgen precursors (41). While we did not observe increased serum 11OHA4
409 concentrations in the current study, we cannot exclude that increased adrenal output of this precursor
410 contributed to the observed increase in 11KT biosynthesis. In fact, this is likely the case as circulating
411 11OHA4 concentrations were not reduced despite inhibition of HSD11B1 and the resulting significant
412 decrease in the 11OHA4/11KA4 ratio. Furthermore, the original clinical trial observed a significant
413 increase in serum DHEAS, a marker of adrenal C19 steroid biosynthesis, thus confirming the stimulation
414 of adrenal steroidogenesis (40). Despite the potential increase in adrenal 11OHA4 biosynthesis, our *in*
415 *vitro*, *ex vivo* and *in silico* data unequivocally show that HSD11B1 modulates the peripheral
416 biosynthesis of 11KT and that inhibition of HSD11B1 results in increased peripheral 11KT production
417 irrespective of adrenal 11OHA4 output.
418 This study highlights that HSD11B1 inhibition may not be as effective as previously anticipated for the
419 treatment of metabolic conditions in women due to the concomitant increase in the active androgen
420 pool. However, the current data does not call into question the safety or efficacy of HSD11B1 inhibitors
421 such as AZD4017, which has been shown to be well tolerated (39–41, 54, 70), but rather highlights that
422 the condition targeted by the use of HSD11B1 inhibitors needs to be carefully considered. To date,
423 AZD4017 has shown promise in the treatment of Idiopathic Intracranial Hypertension and wound
424 healing in adults with type 2 diabetes, thus warranting further studies (40, 41). It may also be
425 interesting to consider HSD11B1 inhibition in oophorectomized women. In this setting, the increased
426 biosynthesis of 11KT due to HSD11B1 inhibition may be beneficial in offsetting the androgen deficiency

427 due to oophorectomy, while reduced local glucocorticoid activation has the potential to protect
428 against glucocorticoid induced osteoporosis, especially against the backdrop of reduced estrogen
429 biosynthesis (71–73).
430 In summary, our findings indicate that HSD11B1 plays an essential role in modulating the amount of
431 11KT produced by AKR1C3 expressed in adipose tissue. As a result, inhibition of HSD11B1 does not just
432 reduce local glucocorticoid activation, but also alters the biosynthesis of the potent 11-oxygenated
433 androgen 11KT. In women, the significant increase in 11KT concentrations may have metabolically
434 opposing effects that attenuate the beneficial reduction of glucocorticoid activation in metabolic
435 tissue. It is therefore imperative that future HSD11B1 inhibitor studies consider both the glucocorticoid
436 and androgen pools and that sex-specific effects are systematically investigated and considered in the
437 design of future studies.

438 **Materials and Methods**

439 **Steroids and inhibitors**

440 Androstenedione (4-androstene-3,17-dione), carbenoxolone ((3β,20β)-3-(3-carboxy-1-oxopropoxy)-
441 11-oxo-olean-12-en-29-oic acid, disodium salt; CBX), cortisol (11β,17α,21-trihydroxypregn-4-ene-3,20-
442 dione), cortisone (17α,21-dihydroxy-4-pregnene-3,11,20-trione), DHEA (5-androsten-3β-ol-17-one),
443 DHEA sulfate (5-androsten-3β-ol-17-one-3-sulfate) and testosterone (4-androsten-17β-ol-3-one) were
444 purchased from Sigma Aldrich. 11β-hydroxyandrostenedione (11β-hydroxy-4-androstene-3,17-dione),
445 11β-hydroxytestosterone (11β,17β-dihydroxyandrost-4-en-3-one), 11-ketoandrostenedione (4-
446 androsten-3,11,17-trione) and 11-ketotestosterone (4-androsten-17β-ol-3,11-dione) were from
447 Steraloids. The deuterated internal standards 11β-hydroxyandrostenedione-2,2,4,6,6,16,16-D7 (D7-
448 11OHA4), 11-ketotestosterone-16,16,17-D3 (D3-11KT), androstenedione-2,2,4,6,6,16,16-D7 (D7-A4),
449 cortisol-9,11,12,12-D4 (D4-F), DHEAS-16,16-D2 (D2-DHEAS) and testosterone-16,16,17-D3 (D3-T) were
450 all purchased from Cambridge Isotope Laboratories. Dehydroepiandrosterone-2,2,3,4,4,6-D6 (D6-
451 DHEA) and cortisone-2,2,4,6,6,9,12,12-D8 (D8-E) were purchased from Sigma Aldrich, while 11-
452 ketoandostenedione-2,2,4,6,6,9,12,12,16,16-D10 (D10-11KA4) was custom synthesized by Toronto
453 Research Chemicals. The selective HSD11B1 inhibitor, 2-[(3S)-1-[5-(cyclohexylcarbamoyl)-6-
454 propylsulfanylpyridin-2-yl]-3-piperidyl] acetic acid (AZD-4017) was provided by AstraZeneca.

455 **Plasmids**

456 The pcDNA3 vector containing AKR1C3 was provided by Prof. J. Adamski (Helmholtz Zentrum
457 München, Germany). The pcDNA3 vectors containing HSD11B1 and hexose 6-phosphate
458 dehydrogenase (H6PDH) were from Prof. K. Chapman (University of Edinburgh, UK). The pTAT-GRE-
459 Elb-luc luciferase promoter reporter construct, containing two copies of the GRE was from Prof. G.
460 Jenster (Erasmus University of Rotterdam, Netherlands), while the GR expressing plasmid (pRShGRα)
461 was from Prof. R. Evans (Howard Hughes Medical Institute, La Jolla, USA). The pCIneo plasmid
462 expressing the wild-type human AR was from Prof. N. Sharifi (Cleveland Clinic, Cleveland, USA). A
463 pCIneo plasmid, containing no cDNA insert, was purchased from Promega (Wisconsin, USA).

464 **Cell lines**

465 HEK293 cells were purchased from the American Type Culture Collections (ATCC) and cultured in high
466 glucose Dulbecco's Modified Eagle Medium (DMEM) supplemented with 10% FBS, 1.5 g/L $NaHCO_3$ and
467 1% penicillin-streptomycin and maintained at 37 °C in 90% humidity and 5% CO^2. The cells were
468 authenticated by short-tandem repeat profiling (NorthGene) and were regularly tested for
469 mycoplasma contamination.

470

471 **Determining kinetic parameters for HSD11B1 and computational model construction**

472 The kinetic parameters ($K_{m,\ app}$ and $V_{max,\ app}$) for HSD11B1 were determined using the methodology
473 previously reported for AKR1C3 (16). Briefly, HEK293 cells were seeded into 10 cm^2 tissue culture
474 dishes at a density of $2x10^5$ cells per mL (10 mL per dish). After a 24 hour incubation period, cells were
475 co-transfected with 0.5 µg HSD11B1 and 0.5 µg H6PDH DNA using X-tremeGENE™ HP DNA transfection
476 reagent (Roche) according to manufacturer's protocol. Following a 24 hour incubation the transfected
477 cells were re-plated into 48-well Corning® CELLBIND® plates at a density of $2x10^5$ cells per mL (300 µL
478 per well). Cells were incubated for an additional 24 hours to allow for attachment before being treated
479 with serum free media, containing appropriate steroid substrate (cortisone, 11KA4, or 11KT) at
480 concentrations ranging from 0.1 µM to 10 µM. Aliquots (250 µL) for the quantification of steroid
481 metabolism by ultra-high performance liquid chromatography tandem mass spectrometry (UHPLC-
482 MS/MS) were collected at specific time intervals. Kinetic parameters were determined in Wolfram
483 Mathematica (Version 13) by assuming Michaelis Menten kinetics and fitting the $K_{m,\ app}$ and $V_{max,\ app}$
484 values by minimizing the sum of the squared differences between the experimentally determined
485 progress curves and model, weighted by the variance using the NMinimize function. The model was
486 fitted to triplicate data from three independent experiments. The transfection efficiency of each
487 individual experiment was taken into account by determining the initial rate of the conversion of 100
488 nM 11KA4 for each independent experiment. A computational model containing the determined
489 kinetic for HSD11B1 and those previously determined for AKR1C3 was subsequently constructed. This
490 model is comprised of ordinary differential equations (ODEs) for the metabolites, and numerical
491 integration by making use of the NDSolve routine in Mathematica allowed for experimentally
492 comparable metabolite profiles to be obtained. Additionally, the model was used to predict the
493 conversion of cortisone or 11KA4 for varying HSD11B1:AKR1C3 ratios, see Supplementary material for
494 a complete model description and simulation details.

495 **Determining the effect of different HSD11B1:AKR1C3 ratios on cortisone and 11KA4 metabolism**

496 HEK293 cells were seeded into 10 cm^2 tissue culture dishes at a density of $2x10^5$ cells per mL (10 mL
497 per dish). After a 24 hour incubation period, dishes were co-transfected with either 0.5 µg HSD11B1
498 and 0.5 µg H6PDH or 0.5 µg AKR1C3 and 0.5 µg pCINeo using X-tremeGENE™ HP DNA transfection
499 reagent (Roche). Additional dishes were transfected with 1 µg of the pCINeo (no insert) as to allow for
500 the subsequent plating of an equal number of transfected cells at all HSD11B1:AKR1C3 ratios. After 24
501 hours cells were counted and combined in different ratios of HSD11B1:AKR1C3, before being re-plated
502 into 12-well Corning® CELLBIND® surface plates at a density of $4x10^5$ cells per mL (1 mL per well). After
503 an additional incubation period of 24 hours, the media was replaced with serum free DMEM containing
504 100 nM substrate (11KA4 or cortisone). Aliquots (500 µL) were collected 24 hours after the addition of
505 substrate for analysis by UHPLC-MS/MS, as described below.

506 **Determining the effect of CBX on HSD11B1 and AKR1C3 co-expression**

507 HSD11B1 and AKR1C3 transfections were performed as described above. Transfected cells were
508 re-plated at a 1:1 ratio of HSD11B1:AKR1C3 ($2x10^5$ cells/mL, 300 µL) in 48-well Corning® CELLBIND®
509 surface plates. After 24 hours, media was replaced with serum free media containing 100 nM cortisone
510 in combination with either 10 nM or 100 nM 11KA4 in the absence and presence of 10 µM CBX.
511 Aliquots (200 µL) were collected over a 24 hour period for analysis by UHPLC-MS/MS.

512 **Promoter reporter assays**

513 To determine the effect of the HSD11B1 inhibitor CBX on AR and GR transactivation, HSD11B1 and
514 AKR1C3 transfections were performed 24 hours before co-transfections of HEK293 cells with either a
515 AR expression plasmid (0.09 µg) and the pTAT-GRE-Elb-luc luciferase promoter reporter construct (0.9
516 µg) or a GR expression plasmid (0.09 µg) and the pTAT-GRE-Elb-luc luciferase promoter reporter
517 construct (0.9 µg). HSD11B1 and AKR1C3 transfected cells were re-plated at a 1:1 ratio ($4x10^5$ cells/mL,
518 1 mL) in 12-well Corning® CELLBIND® surface plates. Following 24 hours, media was replaced with
519 serum free media containing 100 nM cortisone and 10 nM 11KA4 in the absence and presence of 10
520 µM CBX. At the same time the AR-GRE transfected cells and GR-GRE transfected cells were re-plated
521 into 48-well Corning® CELLBIND® plates ($3x10^5$ cells/mL, 300 µL). Following a 24 hour incubation with
522 steroid, aliquots (200 µL) from the HSD11B1:AKR1C3 expressing cells were collected for analysis of
523 steroid metabolism by UHPLC-MS/MS. A further 300 µL conditioned media was transferred to each of
524 the AR-GRE and GR-GRE transfected cells. These cells were incubated for a further 24 hours after which
525 cell lysates were harvested in passive lysis buffer. Reporter activity was then measured by making use
526 of the Luciferase Assay System (Promega). The luciferase values were normalised to the protein
527 concentration of each individual sample determined using a Thermo Scientific™ Pierce™ BCA Protein
528 Assay kit.

529 **Determining the effect of ADZ4017 on 11KA4 conversion in human adipose tissue**

530 Paired subcutaneous and omental adipose tissue was collected from eight female participants (age
531 range 32-59 years, BMI range 42-57 kg/m^2) undergoing elective abdominal non-cancer surgery (Black
532 Country Research Ethics Committee references 14/WM/0011 and 19/WM/0183). Written, informed
533 consent was obtained prior to surgery and sample collection. Adipose tissue samples were transported
534 to the laboratory at room temperature in DMEM/F12 supplemented with 33 µM biotin, 17 µM
535 panthotenic acid and 1% penicillin-streptomycin. Connective tissue and vessels were removed and the
536 adipose tissue washed in PBS. Tissue samples of 100-300 mg were cut and weighed. Each sample was
537 cut into four smaller pieces for incubations with 100 nM cortisone or 100 nM 11KA4 in the presence
538 and absence of 100 nM HSD11B1 inhibitor AZD4017 in DMEM/F12-Ham (supplemented as described
539 above). Final solvent concentrations were adjusted to 0.00302% MeOH and 0.1% DMSO in all
540 incubations. Tissue incubations were constantly rotated in a hybrid oven at 37 °C for 72 hours. Medium
541 samples were centrifuged for 10 minutes at 16,000g and 4 °C and the supernatant was used for analysis
542 of steroid metabolism by UHPLC-MS/MS. The tissue was washed in PBS, snap frozen in liquid nitrogen
543 and stored at -80 °C for RNA extraction.

544 **RNA isolation and gene expression analysis from HEK293 cells**

545 Total RNA was isolated from cells using Tri-Reagent® (Sigma) and cDNA synthesis carried out using the
546 GoScript™ Reverse Transcription System kit (Promega). Quantitative PCR was performed using a Roche
547 LightCycler® 96 rapid thermal cycler instrument and the KAPA SYBR® FAST qPCR Master Mix for
548 LightCycler®. Primer sequences as follows, AKR1C3 (forward) 5'- AGCCAGGTGAGGAACTTTC-3' (74),
549 AKR1C3 (reverse) 5'- ATCACTGTTAAAATAGTGGAG-3' (74), HSD11B1 (forward) 5'-
550 CTGCCTGCTTAGGAGGTTGT-3', HSD11B1 (reverse) 5'- CCTTGGAGCATCTCTGGTCTG-3', the reference
551 gene ubiquitin conjugating enzyme (UBC) (forward) 5'- CCGGGATTTGGGTCGCAG-3', UBC (reverse) 5'-
552 TCACGAAGATCTGCATTGTCAAG-3'. Primer efficiencies were between 90% and 110% for all primer sets.
553 Relative gene expression was calculated using a modified form of the model described by Pfaffl (75).
554 Inter-experimental variations were adjusted using a mean-centering (76).

555 **RNA isolation and gene expression analysis from adipose tissue**

556 Adipose tissue was homogenised in Tri-Reagent® and total RNA was isolated after phenol-chloroform
557 extraction using the Qiagen RNeasy Mini Kit using an established protocol (77). Reverse transcription
558 was performed using Applied Biosystems™ TaqMan™ Reverse Transcription Reagents according to the
559 manufacturer's protocol. qPCR was performed on an ABI 7900HT sequence detection system (Perkin
560 Elmer, Applied Biosystems) using TaqMan™ Gene Expression Assays (FAM-labelled) and the
561 SensiFAST™ Probe Hi-ROX kit (Bioline). The following TaqMan™ Gene Expression Assays were used:
562 18S Hs99999901_s1, AKR1C3 Hs00366267_m1, HSD11B1 Hs01547870_m1.

563 **Determining the effect of ADZ4017 glucocorticoid and androgen concentrations *in vivo***

564 A total of 28 participants (22 male and 6 female), all with type 2 diabetes, were recruited for a
565 randomized, double-blind, parallel-group, placebo-controlled trial. Full ethical approval was acquired
566 from North West Greater Manchester Central Research Ethics Committee 17/NW/0283 prior to the
567 initiation of recruitment for the study. Informed consent was obtained from all participants after the
568 nature and possible consequences of the study had been explained. Participants received either oral
569 AZD4017 (400 mg) or a matched oral placebo twice daily for 35 days. Blood samples and urine were
570 collected from individuals before first treatment and after completion of the trial and were analysed
571 by UHPLC-MS/MS and GC-MS, respectively. Refer to Ajjan *et al.* (40) for further details on study design
572 and participants.

573 **Steroid extraction**

574 Steroids were extracted from HEK293 tissue culture media using Tert-butyl methyl ether (MTBE) (78).
575 In brief, following the addition of an internal standard mix (100 µL containing 2 ng D3-T and 5 ng D7-
576 A4, D7-11OHA4, D3-11KT and D4-F in acetonitrile) and MTBE (3:1 ratio of MTBE:media), samples were
577 vortexed at 1 500 rpm for 10 minutes, after which they were incubated at -80 °C for 1 hour, allowing
578 for the aqueous layer to freeze. The resulting organic phase was subsequently transferred to a clean
579 test tube and evaporated under a stream of nitrogen gas at 45 °C. Extracted steroids were then
580 reconstituted by the addition of 50% (v/v) methanol and stored at -20 °C until analysis by UHPLC-
581 MS/MS. Serum steroids and steroids in medium adipose tissue incubations were extracted using a
582 similar method. Samples (200 µL for serum, 500 µL for adipose tissue conditioned medium) were mixed
583 with 10 µL internal standards in 50% (v/v) methanol in water (D4-F, D8-E, D6-DHEA, D7-A4, D3-T, D7-
584 11OHA4, D10-11KA4, D3-11KT; 5 ng each for serum, 20 ng each for adipose tissue). For serum samples
585 50 µL acetonitrile were added for protein precipitation prior to extraction and the samples vortexed.
586 MTBE was added to each sample (1 mL for serum; 3 mL for medium from adipose tissue incubations)
587 and the samples were vortexed at 1000 rpm for 10 min. Following incubation at room temperature for
588 30 minutes the organic phase was transferred, dried under a stream of nitrogen gas at 45 °C and
589 reconstituted with 50% (v/v) methanol in water prior to analysis by UHPLC-MS/MS. For the
590 measurement of serum DHEAS, 200 ng D2-DHEAS in 20 uL of 50% methanol was added to 20 µL of
591 serum followed by 20 µL of 1 mM $ZnSO_4$ and 100 µL acetonitrile. The samples were centrifuged and
592 100 µL of the supernatant was dried and reconstituted in 50% (v/v) methanol in water prior to UHPLC-
593 MS/MS analysis.

594 **Quantification of steroids by ultra-high performance liquid chromatography tandem mass**
595 **spectrometry (UHPLC-MS/MS)**

596 Steroids from assays performed in HEK293 cells were separated and quantified using a UPLC high
597 strength silica (HSS) T3 column (2.1 mm X 50 mm, 1.8 µm particle size) coupled to an ACQUITY UPLC
598 and Xevo TQ-S triple quadrupole mass spectrometer (Waters Corporation, Milford, USA) as previously
599 reported (78). Steroids extracted from serum or adipose tissue incubations were separated and
600 quantified using Phenomenex Luna Omega polar C18 column (2.1 X 50 mm, 1.6 µm particle size;
601 Phenomenex, Macclesfield, UK) coupled to an ACQUITY UPLC and a Waters Xevo TQ-XS triple
602 quadrupole mass spectrometer as previously described (79). Serum DHEAS was quantified using a HSS
603 T3 column (2.1 X 50 mm, 1.8 µm particle size; Waters) coupled to an ACQUITY UPLC and a Waters Xevo
604 TQ-XS triple quadrupole mass spectrometer as previously described (80, 81).

605 **Quantification of urinary steroids by GC-MS**

606 Measurement of urinary steroid metabolite excretion was carried out by a long-established gas
607 chromatography-mass spectrometry (GC-MS) method (82). In brief, free and conjugated steroids were
608 extracted from 1 mL urine by solid-phase extraction. Steroid conjugates were enzymatically
609 hydrolyzed, reextracted, and chemically derivatized to form methyloxime trimethyl silyl ethers. An
610 Agilent 5975 instrument operating in selected-ion-monitoring (SIM) mode achieved sensitive and
611 specific detection and quantification of selected steroid metabolites.

612 **Statistical analysis**

613 We performed unpaired t-tests to compare the effect of HSD11B1 inhibition on 11-oxygenated
614 androgen production in HEK293 cells expressing AKR1C3 and HSD11B1 and on the transactivation of
615 the androgen receptor. Paired t-tests were performed to assess the effect of HSD11B1 inhibition in
616 adipose tissue, while Wilcoxon signed-rank tests were used to assess the effect in serum and urine.
617 Correlations between serum steroid concentrations and clinical outcomes were investigated using a
618 Spearman's Rho test.

619 **Funding**

620 This work has been supported by the National Research Foundation of South Africa (Grant Number
621 132503, to KHS); the Academy of Medical Sciences UK (Newton Advanced Fellowship NAF004\1002,
622 to KHS); the Wellcome Trust (Investigator Grant WT209492/Z/17/Z, to WA); a Medical Research
623 Council Confidence in Concept Award to AT (MC_PC_15046); and a SARChI DST/NRF grant (82813, to
624 JS).

625 **Author contributions**

626 KHS, WA and LS were responsible for study concept and design. LS and IO conducted experiments. JS
627 performed all computational modelling. LS, IO, JS, LCG, AET, and KHS analysed data. AJC and RS
628 provided human adipose tissue. AT, RA and AF provided serum and urine from a phase 2b pilot trial
629 with AZD4017. AET and LCG conducted the analysis of clinical samples by LC-MS/MS and GC-MS,
630 respectively. KHS, LS and IO drafted the manuscript. WA, AT and JS critically reviewed the manuscript.
631 All authors reviewed and approved the final version of the manuscript. KS and WA obtained funding.
632 These authors contributed equally: LS and IO. LS was selected as the first of the two authors as she
633 was involved in the conceptualisation of the study.

634 **References**

635 1. Pretorius E, Arlt W, Storbeck K-H. A new dawn for androgens: Novel lessons from 11-
636 oxygenated C19 steroids. *Mol. Cell. Endocrinol.* 2017;441:76–85.
637 2. Turcu AF, et al. 11-Oxygenated androgens in health and disease. *Nat. Rev. Endocrinol.*
638 2020;16(5):284–296.
639 3. Schiffer L, et al. Classic and 11-oxygenated androgens in serum and saliva across adulthood: a
640 cross-sectional study analyzing the impact of age, body mass index, and diurnal and menstrual
641 cycle variation. *Eur. J. Endocrinol.* 2023;188(1):1–15.
642 4. Storbeck K-H, O'Reilly MW. The clinical and biochemical significance of 11-oxygenated
643 androgens in human health and disease. *Eur. J. Endocrinol.* [published online ahead of print:
644 April 12, 2023]; doi:10.1093/EJENDO/LVAD047
645 5. Pretorius E, et al. 11-ketotestosterone and 11-ketodihydrotestosterone in castration resistant
646 prostate cancer: potent androgens which can no longer be ignored. *PLoS One*
647 2016;11(7):e0159867.
648 6. Nanba AT, et al. 11-Oxygenated C19 Steroids Do Not Decline with Age in Women. *J. Clin.*
649 *Endocrinol. Metab.* 2019;104(7):2615–2622.
650 7. Skiba MA, et al. Androgens During the Reproductive Years: What Is Normal for Women?. *J Clin*
651 *Endocrinol Metab* 2019;104(11):5382–5392.
652 8. O'Reilly MW, et al. 11-oxygenated C19 steroids are the predominant androgens in polycystic
653 ovary syndrome. *J. Clin. Endocrinol. Metab.* 2017;102(3):840–848.
654 9. Turcu AF, et al. Adrenal-derived 11-oxygenated 19-carbon steroids are the dominant
655 androgens in classic 21-hydroxylase deficiency. *Eur. J. Endocrinol.* 2016;174(5):601–609.
656 10. Nowotny HF, et al. 11-Oxygenated C19 steroids are the predominant androgens responsible
657 for hyperandrogenemia in Cushing's disease. *Eur. J. Endocrinol.* 2022;187(5):663–673.
658 11. Storbeck K-H, et al. 11β-hydroxydihydrotestosterone and 11-ketodihydrotestosterone, novel
659 C19 steroids with androgenic activity: a putative role in castration resistant prostate cancer?.
660 *Mol. Cell. Endocrinol.* 2013;377(1–2):135–146.

661 12. Snaterse G, et al. 11-Ketotestosterone is the predominant active androgen in prostate cancer
662 patients after castration. *JCI Insight* 2021;6(11):e148507.
663 13. Storbeck K-H. A commentary on the origins of 11-ketotestosterone. *Eur J Endocrinol*
664 2022;187(6):C5-8.
665 14. Quinkler M, et al. Androgen generation in adipose tissue in women with simple obesity - A
666 site-specific role for 17β-hydroxysteroid dehydrogenase type 5. *J. Endocrinol.*
667 2004;183(2):331–342.
668 15. O'Reilly MW, et al. AKR1C3-Mediated Adipose Androgen Generation Drives Lipotoxicity in
669 Women With Polycystic Ovary Syndrome. *J Clin Endocrinol Metab* 2017;102(9):3327–3339.
670 16. Barnard M, et al. 11-Oxygenated androgen precursors are the preferred substrates for aldo-
671 keto reductase 1C3 (AKR1C3): Implications for castration resistant prostate cancer. *J. Steroid*
672 *Biochem. Mol. Biol.* 2018;183:192–201.
673 17. Paulukinas RD, Mesaros CA, Penning TM. Conversion of Classical and 11-oxygenated
674 Androgens by Insulin Induced AKR1C3 in a Model of Human PCOS Adipocytes. *Endocrinology*
675 2022;163(7):bqac068.
676 18. Tomlinson JW, et al. 11beta-hydroxysteroid dehydrogenase type 1: a tissue-specific regulator
677 of glucocorticoid response. *Endocr Rev* 2004;25(5):831–866.
678 19. Gathercole LL, et al. 11β-Hydroxysteroid Dehydrogenase 1: Translational and Therapeutic
679 Aspects. *Endocr. Rev.* 2013;34(4):525–555.
680 20. Gent R, et al. The 11β-hydroxysteroid dehydrogenase isoforms: pivotal catalytic activities yield
681 potent C11-oxy C 19 steroids with 11βHSD2 favouring 11-ketotestosterone, 11-
682 ketoandrostenedione and 11-ketoprogesterone biosynthesis. *J. Steroid Biochem. Mol. Biol.*
683 2019;189:116–126.
684 21. Morgan SA, et al. 11β-HSD1 is the major regulator of the tissue-specific effects of circulating
685 glucocorticoid excess. *Proc. Natl. Acad. Sci. U. S. A.* 2014;111(24):E2482–E2491.
686 22. Gregory S, et al. 11β-hydroxysteroid dehydrogenase type 1 inhibitor use in human disease-a
687 systematic review and narrative synthesis. *Metabolism.* 2020;108:154246.

688 23. Tiganescu A, et al. Topical 11β-Hydroxysteroid Dehydrogenase Type 1 Inhibition Corrects
689 Cutaneous Features of Systemic Glucocorticoid Excess in Female Mice. *Endocrinology*
690 2018;159(1):547–556.
691 24. Doig CL, et al. 11β-HSD1 Modulates the Set Point of Brown Adipose Tissue Response to
692 Glucocorticoids in Male Mice. *Endocrinology* 2017;158(6):1964–1976.
693 25. Masuzaki H, et al. A transgenic model of visceral obesity and the metabolic syndrome. *Science*
694 2001;294(5549):2166–2170.
695 26. Masuzaki H, et al. Transgenic amplification of glucocorticoid action in adipose tissue causes
696 high blood pressure in mice. *J. Clin. Invest.* 2003;112(1):83–90.
697 27. Kotelevtsev Y, et al. 11beta-hydroxysteroid dehydrogenase type 1 knockout mice show
698 attenuated glucocorticoid-inducible responses and resist hyperglycemia on obesity or stress.
699 *Proc. Natl. Acad. Sci. U. S. A.* 1997;94(26):14924–9.
700 28. Hermanowski-Vosatka A, et al. 11β-HSD1 inhibition ameliorates metabolic syndrome and
701 prevents progression of atherosclerosis in mice. *J. Exp. Med.* 2005;202(4):517–527.
702 29. Morgan SA, et al. 11β-HSD1 contributes to age-related metabolic decline in male mice. *J.*
703 *Endocrinol.* 2022;255(3):117–129.
704 30. Rege J, et al. Circulating 11-oxygenated androgens across species. *J. Steroid Biochem. Mol.*
705 *Biol.* 2019;190:242–249.
706 31. Walker BR, et al. Carbenoxolone increases hepatic insulin sensitivity in man: a novel role for
707 11-oxosteroid reductase in enhancing glucocorticoid receptor activation. *J. Clin. Endocrinol.*
708 *Metab.* 1995;80(11):3155–3159.
709 32. Andrews RC, Rooyackers O, Walker BR. Effects of the 11 beta-hydroxysteroid dehydrogenase
710 inhibitor carbenoxolone on insulin sensitivity in men with type 2 diabetes. *J. Clin. Endocrinol.*
711 *Metab.* 2003;88(1):285–291.
712 33. Sandeep TC, et al. Increased in vivo regeneration of cortisol in adipose tissue in human obesity
713 and effects of the 11beta-hydroxysteroid dehydrogenase type 1 inhibitor carbenoxolone.
714 *Diabetes* 2005;54(3):872–879.

715 34. Rosenstock J, et al. The 11-beta-hydroxysteroid dehydrogenase type 1 inhibitor INCB13739
716 improves hyperglycemia in patients with type 2 diabetes inadequately controlled by
717 metformin monotherapy. *Diabetes Care* 2010;33(7):1516–1522.
718 35. Feig PU, et al. Effects of an 11β-hydroxysteroid dehydrogenase type 1 inhibitor, MK-0916, in
719 patients with type 2 diabetes mellitus and metabolic syndrome. *Diabetes. Obes. Metab.*
720 2011;13(6):498–504.
721 36. Shah S, et al. Efficacy and safety of the selective 11β-HSD-1 inhibitors MK-0736 and MK-0916
722 in overweight and obese patients with hypertension. *J. Am. Soc. Hypertens.* 2011;5(3):166–
723 176.
724 37. Heise T, et al. Safety, efficacy and weight effect of two 11β-HSD1 inhibitors in metformin-
725 treated patients with type 2 diabetes. *Diabetes. Obes. Metab.* 2014;16(11):1070–1077.
726 38. Yadav Y, et al. Inhibition of 11β-Hydroxysteroid dehydrogenase-1 with AZD4017 in patients
727 with nonalcoholic steatohepatitis or nonalcoholic fatty liver disease: A randomized, double-
728 blind, placebo-controlled, phase II study. *Diabetes. Obes. Metab.* 2022;24(5):881–890.
729 39. Abbas A, et al. Effect of AZD4017, a Selective 11β-HSD1 Inhibitor, on Bone Turnover Markers
730 in Postmenopausal Osteopenia. *J. Clin. Endocrinol. Metab.* 2022;107(7):2026–2035.
731 40. Ajjan RA, et al. Oral 11β-HSD1 inhibitor AZD4017 improves wound healing and skin integrity in
732 adults with type 2 diabetes mellitus: a pilot randomized controlled trial. *Eur. J. Endocrinol.*
733 2022;186(4):441–455.
734 41. Hardy RS, et al. 11βHSD1 Inhibition with AZD4017 Improves Lipid Profiles and Lean Muscle
735 Mass in Idiopathic Intracranial Hypertension. *J. Clin. Endocrinol. Metab.* 2021;106(1):174–187.
736 42. Bianzano S, et al. Safety, tolerability, pharmacodynamics and pharmacokinetics following
737 once-daily doses of BI 187004, an inhibitor of 11 beta-hydroxysteroid dehydrogenase-1, over
738 28 days in patients with type 2 diabetes mellitus and overweight or obesity. *Diabetes, Obes.*
739 *Metab.* 2023;25(3):832–843.
740 43. O'Reilly MW, et al. Serum testosterone, sex hormone-binding globulin and sex-specific risk of
741 incident type 2 diabetes in a retrospective primary care cohort. *Clin. Endocrinol. (Oxf).*

742 2019;90(1):145–154.
743 44. Fauser BCJM, et al. Revised 2003 consensus on diagnostic criteria and long-term health risks
744 related to polycystic ovary syndrome (PCOS). *Hum. Reprod.* 2004;19(1):41–47.
745 45. Legro RS, et al. Diagnosis and treatment of polycystic ovary syndrome: An endocrine society
746 clinical practice guideline. *J. Clin. Endocrinol. Metab.* 2013;98(12):4565–4592.
747 46. McCartney CR, Marshall JC. Polycystic Ovary Syndrome. *N. Engl. J. Med.* 2016;375(1):54–64.
748 47. Legro RS, et al. Prevalence and Predictors of Risk for Type 2 Diabetes Mellitus and Impaired
749 Glucose Tolerance in Polycystic Ovary Syndrome: A Prospective, Controlled Study in 254
750 Affected Women. *J. Clin. Endocrinol. Metab.* 1999;84(1):165–169.
751 48. Randeva HS, et al. Cardiometabolic Aspects of the Polycystic Ovary Syndrome. *Endocr. Rev.*
752 2012;33(5):812–841.
753 49. Jones H, et al. Polycystic ovary syndrome with hyperandrogenism is characterized by an
754 increased risk of hepatic steatosis compared to nonhyperandrogenic PCOS phenotypes and
755 healthy controls, independent of obesity and insulin resistance. *J. Clin. Endocrinol. Metab.*
756 2012;97(10):3709–3716.
757 50. Rocha ALL, et al. Non-alcoholic fatty liver disease in women with polycystic ovary syndrome:
758 systematic review and meta-analysis. *J. Endocrinol. Invest.* 2017;40(12):1279–1288.
759 51. Cai J, et al. High-free androgen index is associated with increased risk of non-alcoholic fatty
760 liver disease in women with polycystic ovary syndrome, independent of obesity and insulin
761 resistance. *Int. J. Obes.* 2017;41(9):1341–1347.
762 52. Kumarendran B, et al. Polycystic ovary syndrome, androgen excess, and the risk of
763 nonalcoholic fatty liver disease in women: A longitudinal study based on a United Kingdom
764 primary care database. *PLOS Med.* 2018;15(3):e1002542.
765 53. Snaterse G, et al. Androgen receptor mutations modulate activation by 11-oxygenated
766 androgens and glucocorticoids. *Prostate Cancer Prostatic Dis.* [published online ahead of
767 print: January 19, 2022]; doi:10.1038/s41391-022-00491-z
768 54. Scott JS, et al. Discovery of a potent, selective, and orally bioavailable acidic 11β-

769 hydroxysteroid dehydrogenase type 1 (11β-HSD1) inhibitor: discovery of 2-[(3S)-1-[5-
770 (cyclohexylcarbamoyl)-6-propylsulfanylpyridin-2-yl]-3-piperidyl]acetic acid (AZD4017). *J. Med.*
771 *Chem.* 2012;55(12):5951–5964.
772 55. Barnard L, et al. The A-ring reduction of 11-ketotestosterone is efficiently catalysed by
773 AKR1D1 and SRD5A2 but not SRD5A1. *J. Steroid Biochem. Mol. Biol.* 2020;202:105724.
774 56. Davio A, et al. Sex Differences in 11-Oxygenated Androgen Patterns Across Adulthood. *J. Clin.*
775 *Endocrinol. Metab.* 2020;105(8):e2921–e2929.
776 57. Skiba MA, et al. Androgens During the Reproductive Years: What Is Normal for Women?. *J.*
777 *Clin. Endocrinol. Metab.* 2019;104(11):5382–5392.
778 58. Handelsman DJ, Cooper ER, Heather AK. Bioactivity of 11 keto and hydroxy androgens in yeast
779 and mammalian host cells. *J. Steroid Biochem. Mol. Biol.* 2022;218:106049.
780 59. Legro RS, et al. Diagnosis and Treatment of Polycystic Ovary Syndrome: An Endocrine Society
781 Clinical Practice Guideline. *J. Clin. Endocrinol. Metab.* 2013;98(12):4565–4592.
782 60. O'Reilly MW, et al. Hyperandrogenemia predicts metabolic phenotype in polycystic ovary
783 syndrome: The utility of serum androstenedione. *J. Clin. Endocrinol. Metab.* 2014;99(3):1027–
784 1036.
785 61. Schiffer L, et al. MECHANISMS IN ENDOCRINOLOGY: The sexually dimorphic role of androgens
786 in human metabolic disease. *Eur. J. Endocrinol.* 2017;177(3):R125–R143.
787 62. Kempegowda P, et al. Implicating androgen excess in propagating metabolic disease in
788 polycystic ovary syndrome. *Ther. Adv. Endocrinol. Metab.* 2020;11:2042018820934319.
789 63. Oda S, et al. An Open-label Phase I/IIa Clinical Trial of 11β-HSD1 Inhibitor for Cushing's
790 Syndrome and Autonomous Cortisol Secretion. *J. Clin. Endocrinol. Metab.*
791 2021;106(10):E3865–E3880.
792 64. Prete A, et al. Cardiometabolic Disease Burden and Steroid Excretion in Benign Adrenal
793 Tumors : A Cross-Sectional Multicenter Study. *Ann. Intern. Med.* 2022;175(3):325–334.
794 65. Zhu L, et al. Testosterone stimulates adipose tissue 11beta-hydroxysteroid dehydrogenase
795 type 1 expression in a depot-specific manner in children. *J. Clin. Endocrinol. Metab.*

796 2010;95(7):3300–3308.
797 66. Pivonello R, et al. Metabolic disorders and male hypogonadotropic hypogonadism. *Front.*
798 *Endocrinol. (Lausanne).* 2019;10:345.
799 67. Kroon J, Pereira AM, Meijer OC. Glucocorticoid Sexual Dimorphism in Metabolism: Dissecting
800 the Role of Sex Hormones. *Trends Endocrinol. Metab.* 2020;31(5):357–367.
801 68. Ruiz D, Padmanabhan V, Sargis RM. Stress, sex, and sugar: Glucocorticoids and sex-steroid
802 crosstalk in the sex-specific misprogramming of metabolism. *J. Endocr. Soc.*
803 2020;4(8):bvaa087.
804 69. Kaikaew K, Grefhorst A, Visser JA. Sex Differences in Brown Adipose Tissue Function: Sex
805 Hormones, Glucocorticoids, and Their Crosstalk. *Front. Endocrinol. (Lausanne).* 2021;12:357.
806 70. Markey K, et al. 11β-Hydroxysteroid dehydrogenase type 1 inhibition in idiopathic intracranial
807 hypertension: a double-blind randomized controlled trial. *Brain Commun.* 2020;2(1):fcz050.
808 71. Shifren JL. Androgen deficiency in the oophorectomized woman. *Fertil. Steril.* 2002;77(SUPPL.
809 4):60–62.
810 72. Stanczyk FZ, et al. Circulating androgen levels before and after oophorectomy in
811 premenopausal and postmenopausal women. *Climacteric* 2019;22(2):169–174.
812 73. Hardy RS, et al. Glucocorticoids and Bone: Consequences of Endogenous and Exogenous
813 Excess and Replacement Therapy. *Endocr. Rev.* 2018;39(5):519–548.
814 74. Matsuura K, et al. Identification of a Principal mRNA Species for Human 3 -Hydroxysteroid
815 Dehydrogenase Isoform (AKR1C3) That Exhibits High Prostaglandin D2 11-Ketoreductase
816 Activity. *J. Biochem.* 1998;124(5):940–946.
817 75. Pfaffl MW. A new mathematical model for relative quantification in real-time RT-PCR. *Nucleic*
818 *Acids Res.* 2001;29(9):e45.
819 76. Willems E, Leyns L, Vandesompele J. Standardization of real-time PCR gene expression data
820 from independent biological replicates. *Anal. Biochem.* 2008;379(1):127–129.
821 77. Guan H, Yang K. RNA isolation and real-time quantitative RT-PCR. *Methods Mol. Biol.*
822 2008;456:259–270.

823 78. Quanson JL, et al. High-throughput analysis of 19 endogenous androgenic steroids by ultra-
824 performance convergence chromatography tandem mass spectrometry. *J. Chromatogr. B*
825 *Anal. Technol. Biomed. Life Sci.* 2016;1031:131–138.
826 79. Schiffer L, et al. Multi-steroid profiling by UHPLC-MS/MS with post-column infusion of
827 ammonium fluoride. *J. Chromatogr. B Anal. Technol. Biomed. Life Sci.* 2022;1209:123413.
828 80. Foster MA, et al. Mapping the Steroid Response to Major Trauma From Injury to Recovery: A
829 Prospective Cohort Study. *J. Clin. Endocrinol. Metab.* 2020;105(3):925–937.
830 81. Chadwick CA, Owen LJ, Keevil BG. Development of a method for the measurement of
831 dehydroepiandrosterone sulphate by liquid chromatography-tandem mass spectrometry.
832 *Ann. Clin. Biochem.* 2005;42(6):468–474.
833 82. Shackleton CHL. Profiling steroid hormones and urinary steroids. *J Chromatogr* 1986;379:91–
834 156.
835